Universitat Politècnica de Catalunya (UPC)
Universitat Autònoma de Barcelona (UAB)
Universitat de Barcelona (UB)
Institut de Ciències Fotòniques (ICFO)

http://www.photonicsbcn.eu

Master in Photonics

MASTER THESIS WORK

Design and fabrication of a lab-on-chip for cell-based waveguides

Tobias Nils Ackermann

Supervised by Dr. Xavier Muñoz Berbel, (IMB-CNM, CSIC)

Presented on date 9th September 2013

Registered at

Escola Tècnica Superior d'Enginyeria de Telecomunicació de Barcelona

Design and fabrication of a lab-on-chip for cell-based waveguides

Tobias Nils Ackermann

Grupo de transductores químicos, GTQ, IMB-CNM (CSIC), Campus UAB, 08193 Cerdanyola del Valles (Barcelona)

Abstract.

The aim of this project was the development of a polymer-based lab-on-chip integrating cell-based waveguides for CVD risk prevention. Cells will have the dual role of transducer and reporter. In order to obtain light-guidance inside the cells, a special set of conditions has to be fulfilled. In this work, this set of conditions was explored for a mono-layer of vascular endothelial cells and a lab-on-chip meeting those requirements was designed.

Keywords: lab-on-a-chip, waveguide, taper, bio-polymers, micro-fluidics

1. Introduction

Cardiovascular disease (CVD) is the leading cause of mortality in Europe, with an estimated cost of 196 billion euros a year [1]. Several potential bio-markers have attracted attention for predictive purposes [2]. However, due to low sensitivity and specificity [2] and rather unclear real predictive value [3], the individual bio-markers only add moderately to the ability of classic vascular risk factors.

Another predictor of CVD is endothelial dysfunction, which makes endothelial cells (ECs) the main subject of interest in the prediction of future cardiac events.

Besides other methods for detection of endothelial dysfunction, direct interrogation of ECs is a very promising strategy. Electrochemical methods [4] and particularly optical measurements in the visible wavelength range are a very interesting tool because they are non-invasive, thus allowing in vivo studies.

From an optical point of view, a cell-culture or tissue can be understood as a bio-material with certain optical properties in terms of refractive index and spectral response. Vascular endothelial dysfunction should be accompanied by physiological and morphological changes. Such changes would alter the optical properties of the ECs and thus may be used in a novel approach to predict future cardiovascular events. Endothelial mono-layers as optical elements, i. e. waveguides (WGs), and thus assigned the dual role of transducer and reporter (living waveguides), could provide very specific

spectral information as a diagnostic tool, indicating changes in the constitution and condition of the cells.

2. Fundamental aspects

Vascular ECs are mammalian cells that proliferate adhered to a suitable substrate [5]. For experimental purposes, they are therefore usually cultured in a fluidic system with a controlled flow pattern providing the required physiological conditions. ECs, e. g. human umbilical vein EC (HUVEC), are isolated from the umbilical vein and umbilical cord blood [6] and injected into the fluidic system. Once inside, they sediment to the bottom of the fluidic channel, where they adhere to the substrate (cell seeding) and start to form a mono-layer of interconnected cells with lateral dimensions determined by the channel-width and -length.

The resultant mono-layer has an average refractive index (RI) of 1.335 and a height of up to 5 µm. These properties cause two major problems in order to really get the mono-layer to act as a living waveguide (LWG). First, the extremely low refractive index of the cells (very similar to that of water) makes it difficult to find a material which supports guided modes inside the cell-layer. And second, the coupling of light into a layer of only few micrometers height with minimal insertion loss has to be achieved.

The following sections present approaches to settle these issues.

2.1. Confinement

Waveguiding is based on total internal reflection. Light can only be totally internally reflected at an interface, if the RI of the material, in which it is travelling, is higher than that of the material at the other side of the interface. For the concrete situation of the endothelial cells in a micro-fluidic channel that requires a RI-profile like the one in Figure 1, defining core and cladding of the LWG. The RI of the ECs, n_{cells}, has to be higher than both n_{medium} and $n_{support}$. For the upper cladding this condition is met, as the cells have a RI slightly higher than the culture medium with $n_{medium} \leq 1.333$. Guided modes for that same RI contrast have already been demonstrated in the infra-red [8].

So the main challenge here is to find a material for the fluidic part of the lab-on-

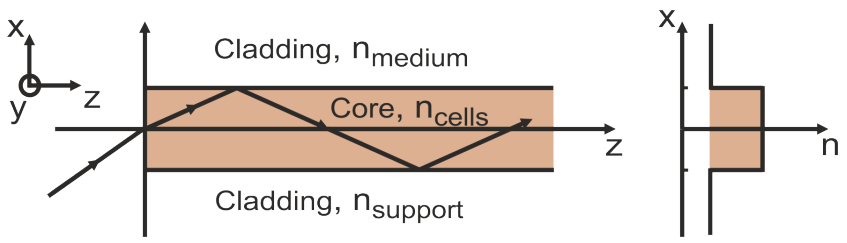

Figure 1. Scheme of total internal reflection and refractive index profile inside a slab-waveguide (based on [7]). Light is confined inside the core given that both cladding layers have a lower refractive index.

chip, which is suitable for cell-culturing and at the same time has a RI low enough to act as lower cladding of the LWG. The polymers well established for the fabrication of both micro-fluidic and micro-optic elements using soft lithography methods, e. g. PDMS (n = 1.41), PEG (n = 1.465) or pHEMA (n = 1.51), have a refractive index much higher than that of cells. For this reason, we propose the use of alternative polymers with RI at least similar to that of water, preferably smaller.

2.2. Coupling

Given a LWG, the main remaining challenge is to efficiently couple light into it. Light coming from a standard multi-mode optical fiber of 50 µm core- and 125 µm cladding-diameter has to enter a front facet of only few µm in height. This approximate size-relation is shown in Figure 2. Hence, to minimize insertion losses, sub-micrometer accuracy in the alignment is necessary and the modal profile of the incident light has to be transformed so as to match the dimensions of the LWG.

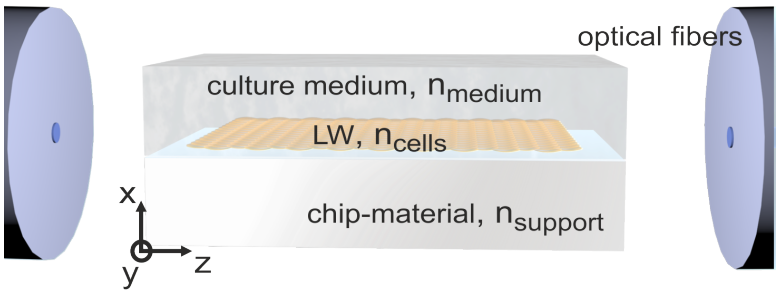

Figure 2. Scheme of an endothelial cell mono-layer inside a micro-fluidic channel grown on a support-material with certain refractive index $n_{support}$ and covered by culture medium with n_{medium}. Standard optical fibers (50 µm core- and 125 µm cladding-diameter) are added to stress the size-relation.

The strategy followed up here to achieve the necessary mode-shrinking and -conversion was to define an integrated tapered waveguide structure. Direct integration into the micro-fluidic platform guarantees excellent alignment. The low RI material required for the fluidic part of the chip promotes the creation of integrated waveguide structures via injection molding, as commonly used polymers like PDMS ($n = 1.41$) or SU-8 ($n = 1.58$) offer high RI contrast. SU-8 is preferable both because of its high RI and its high rigidity, which avoids malfunction caused by eventual bending.

3. Results and discussion

3.1. Confinement and modal profiles of living waveguides

To get an idea of how light will propagate through a EC mono-layer (LWG), mode-matching numerical simulations have been carried out with the software-component

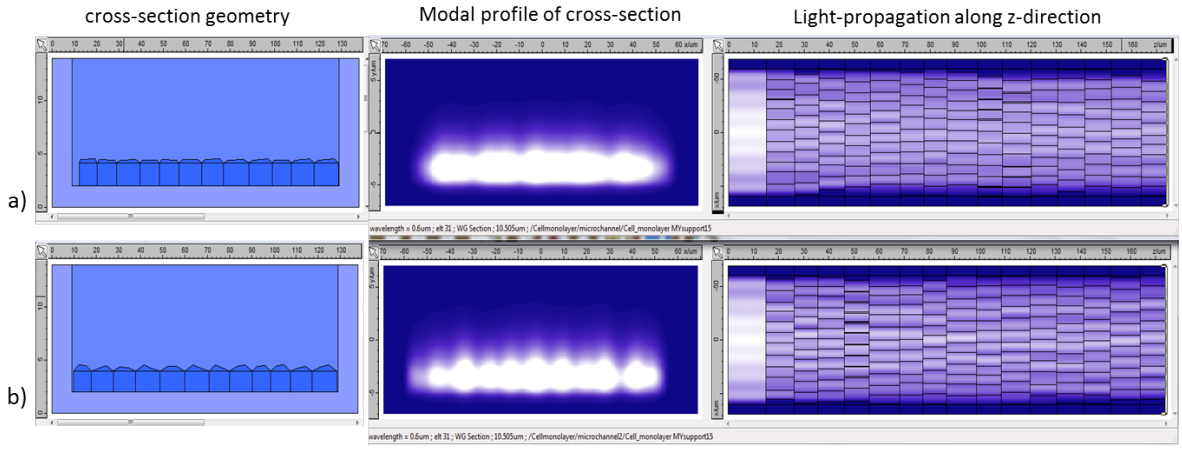

Figure 3. Modelling of light propagation through single layer living photonics. Rows correspond to cell-layers with height fluctuations of up to a) 0.2 µm and b) 0.4 µm. In the first column a representative example of the cross-sectional model geometry with RIs of $n_{cells} = 1.335$, $n_{support} = 1.32$ and $n_{medium} = 1.333$ is shown for each case. The second column contains the calculated respective modal profiles, the third the light distribution along the cell-layer in top-view.

FIMMPROP of Photon Design, a commercially available software designed for the calculation of mode-propagation in waveguides. The results are summarized in Figure 3.

Two planar waveguides with different surface-roughness were implemented in order to model the influence of morphological changes in an EC mono-layer. ECs adhered to the bottom of the micro-fluidic channel are resembled by rectangles of certain constant height, which have trapezoids of random shape on top to simulate height fluctuations. The left column of Figure 3 contains an example of the respective geometries of the model cross-section. The different colors within the cross-section indicate the difference in RI. The RI of the cells was assumed to be $n_{cells} = 1.335$, the RI of the culture medium as the upper cladding $n_{medium} = 1.333$. Bottom and side-walls of the fluidic channel were considered to have a RI of $n_{support} = 1.32$, which is well below the one of the cells. Both LWGs are between 2 and 2.6 µm in height. The one in Figure 3 a) exhibits height fluctuations of up to 0.2 µm, the one in Figure 3 b) up to 0.4 µm. The individual cells with widths between 8 µm and 12 µm were subsequently placed inside the channel, finally forming a row of connected cells.

In both cases, fifteen consecutive rows of varying appearance were then inserted in z-direction with random length between 8 and 12 µm, resulting in a model LWG of around 150 µm length as it is shown in the third column of Figure 3. Light was coupled into the 'device' through a simple slab-waveguide without roughness (corresponding to the first slice in the top-view) of 2 µm height in order to model the coupling by an aligned integrated waveguide matching the dimensions of the LWG. The second and third columns of Figure 3 contain a field plot of light of 532 nm wavelength traveling along the structure, calculated by FIMMPROP. The wavelength was chosen because it is in the middle of the visible spectrum. As expected, the results show rather strong

confinement at the cell-support-interface, but considerable penetration into the liquid medium, as the RI difference is smaller there. Comparing row a) and b) it is obvious that the modal profile is adjusting to the shape-variations introduced by the height-fluctuations. This results also in a difference in transmitted power. For smaller surface-roughness, around 45% of the initial power reaches the end-facet, 37% in the other case. These results suggest, that morphological changes will result in changes of the spectral response, as for different wavelengths different modes are available and transmittance will be affected differently.

3.2. Coupling with an integrated tapered waveguide

An integrated tapered waveguide with an initial width of 50 µm and a final width of 2 µm has been designed and optimized for operation in the visible domain (400-750 nm). Simulations and optimization have been carried out with the respective software-components FIMMPROP and KALLISTOS of Photon Design. A taper-solver with a special algorithm for the near-adiabatic regime was applied, which dynamically splits the structure in successively smaller subsections and interpolates the overlap integrals through those sections.

The final results for optimized shape and length (2730 µm) of the taper, given the constituting RIs of $n = 1.58$ (e. g. SU-8) and $n = 1.32$ respectively, are presented in Figure 4. The spectral response is plotted as percentage of transmitted light staying in the fundamental mode, as a function of the in-coupled wavelength (between 400

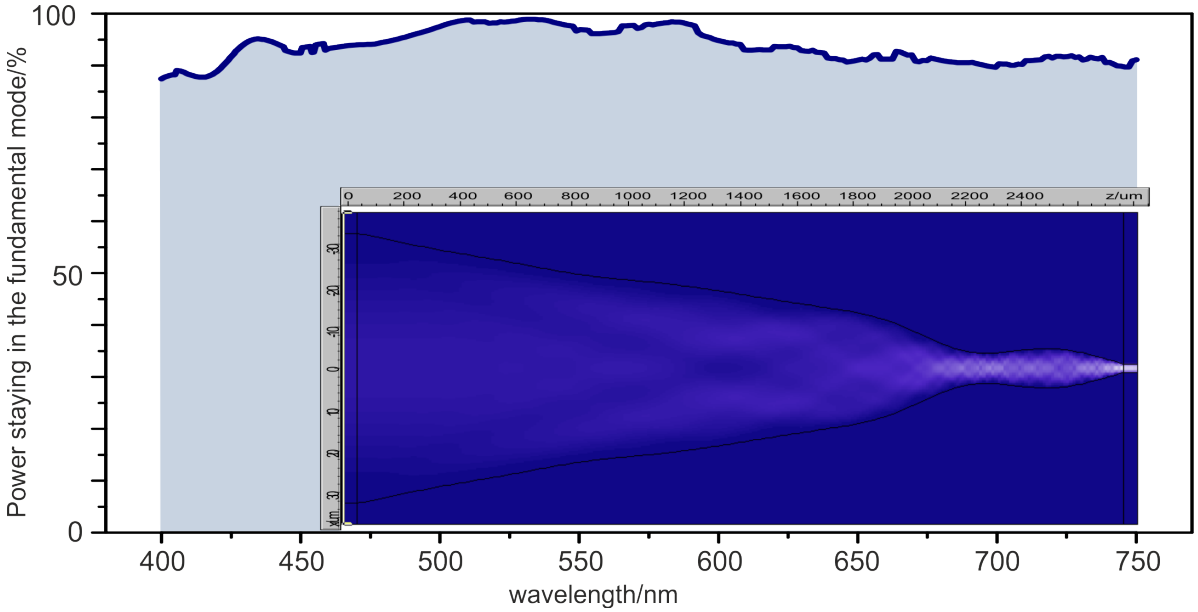

Figure 4. Spectral response of optimized taper shape calculated with Photon Design in the wavelength range from 400 nm to 750 nm. The inset displays the taper shape with width decreasing from 50 µm at z = 0 to 2 µm at z = 2730 µm. A field plot visualizes the light being confined to the tip of the taper.

and 750 nm). According to the calculations, more than 85 % of the in-coupled light stays in the fundamental mode throughout the spectrum, with a maximum of almost 98 % around 532 nm. The inset is a field-plot (at 532 nm), which visualizes how the light is confined in the tip of the taper and efficiently transmitted through a straight continuation of 50 µm length and cross-sectional dimensions (2 µm in height, which here corresponds to the y-axis, and arbitrary width) similar to the expected LWG.

3.3. Lab-on-chip design

Based on the prior considerations, a lab-on-chip for the implementation of LWGs was developed. Regarding the design of the lab-on-chip, both requirements, waveguide-optics, i. e. confinement and coupling and cell-culturing need to be taken into account. Furthermore, the fabrication technique applied comes with certain limitations. The planar technologies used in soft lithography restrict geometries of optical elements to one plane and light will be focused in a plane perpendicular to said plane. Cell seeding however will be driven by gravity. So the design had to ensure, that the EC mono-layers will grow in plane with the focal plane of the integrated micro-optics. The 3-D model in Figure 5 is an extrusion of the CAD-file, according to which the back of the chip will be fabricated. The chip contains a micro-fluidic channel (5) with a straight part of

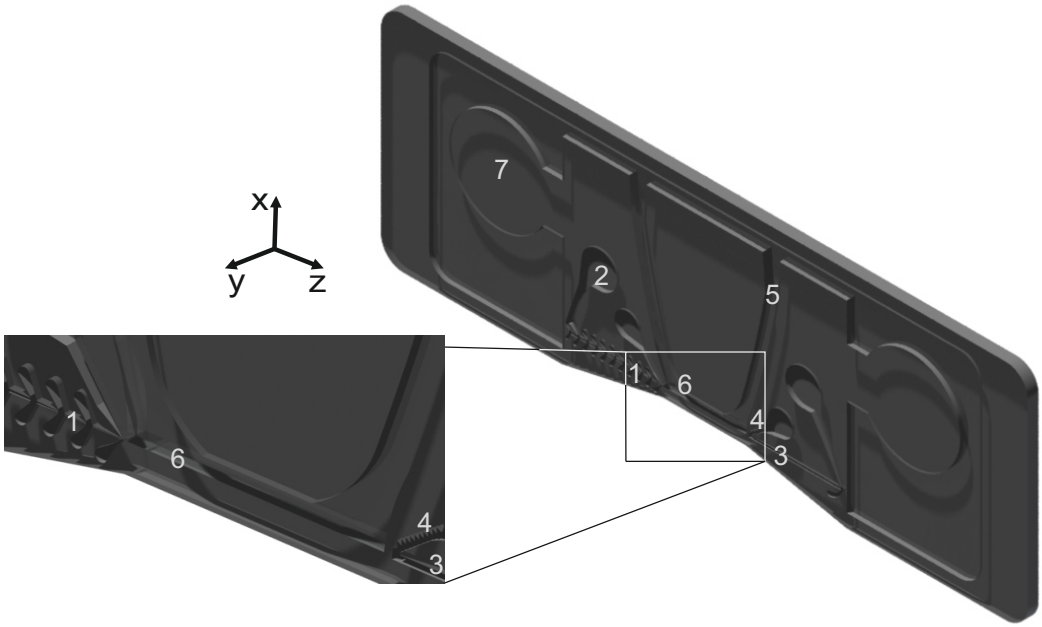

Figure 5. Back part of lab-on-chip for implementing living photonics. (1) Integrated tapered waveguide for in-coupling of light into the living photonics. (2) Insertion sites for injection molding. (3) Integrated waveguide for collecting the output. (4) Triangular grating with arbitrary angles to prevent noise from entering the output WG. (5) Fluidic channel. (6) Interrogation site, cells settle here and grow forming a mono-layer. (7) Auto-alignment structures.

1 mm length (6) between two integrated waveguides (1) and (3). The cells are supposed to grow on the bottom (y-z-plane) of said straight part, forming the living waveguide. Light is in-coupled by a tapered waveguide (1) with a shape according to the simulation-results presented in Figure 4. Due to the fabrication method, the width of the taper (in y-direction) and the micro-fluidic channel are the same and a matched modal profile is achieved. For commonly used channel-widths (y-direction) of more than 125 µm, the tip of the tapered waveguide will have a very high aspect-ratio. Therefore, stabilizing structures were added at the sides. They are pointing against the direction of light propagation in order to minimize interference. In order to investigate the performance of the taper, it will be fabricated also independently from the micro-fluidics.

The rounded extensions at both ends (2) are insertion sites for the injection molding. The straight integrated waveguide (3) at the opposite end of the interrogation site was added for collecting the output of the living waveguide. A triangular grating (4) was added to the insertion extension in order to prevent noise in form of scattered light or light coupled to radiation-modes from entering the output WG. The front part of the chip, which is not shown here, contains self-alignment channels for insertion of optical fibers and closes the micro-fluidic channel. The rounded structures at both sides of the channel (7), of which the front part contains the negatives, play the double role of ensuring alignment of the two parts of the chip and increase the surface-area in order to improve bonding.

This chip-design in principle copes with all the challenges previously discussed and allows the implementation of LWGs. However, a bio-compatible material with appropriate RI and properties suitable for structuring with soft lithography is needed.

3.4. Fabrication of micro-structures with low refractive index bio-polymer

Alternative polymers with RIs of n = 1.32 and n = 1.33 respectively have been found in MY-132A and MY-133-V2000 (fabricated by MY Polymers LTD) [9]. The UV-curable polymers are distributed as adhesives for bio-applications, micro-structuring however has not been done before. For improved adhesion on glass or plastic, the manufacturer provides the primers Primer G and Primer P respectively. Figure 6 displays the first micro-structures obtained with MY-polymers.

Figure 6 b) is a microscope-image of a pillar-structure of MY-132A, which was created by injection molding on a PDMS-substrate using a PDMS-mold fabricated with soft lithography. The substrate was previously coated (using a paint brush) with Primer G. The surface-roughness visible in Figure 6 is created by said coating, but could be essentially reduced by the use of an air-brush. The central pillar is 650 µm, the arms leading to the rounded injection sites 160 µm wide and the whole structure is 125 µm high. The fabrication of micro-structures of both MY-132A and MY-133-V200 has been successfully tested on glass- and PDMS-substrates with and without primers. A crucial point is to avoid the exposure to air during the curing, which can be achieved by nitrogen-atmosphere or curing under water. The manufacturer recommends a dose

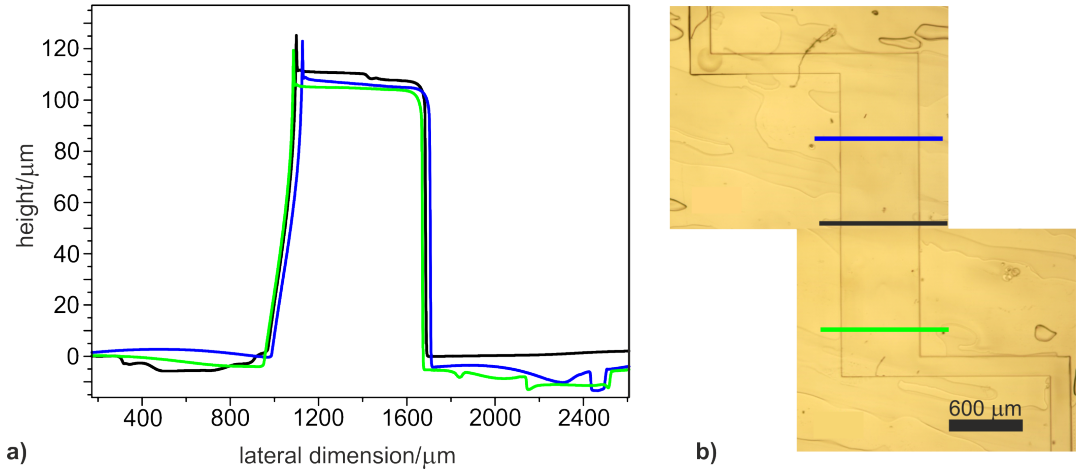

Figure 6. Mechanical height-profile (a) and microscope-image (b) of a pillar-structure obtained with MY-132A. Measurements were taken at three different positions across the central piece of the structure, indicated by the three lines in b).

of at least 4 J/cm^2 [9]. Curing under water however, has been found to require at least 6 J/cm^2. A mechanically obtained height-profile of the structure in Figure 6 b) confirms vertical walls and thus excellent performance of the molding-procedure. The results shown in Figure 6 a) correspond to measurements of the height profile of the central piece of the structure at three different positions, indicated by the three lines across the pillar in Figure 6 b). Probes of both polymers have been provided to partner institutes for tests concerning cell-culturing, final results however are still pending.

3.5. Bio-polymers as model-waveguides

Pillar-structures of MY-133-V200 on MY-132A support are a model system well resembling the preferred RI profile of the bio-waveguides and thus serves for a first proof-of-concept experiment. The model system (see inset in Figure 7 a) was fabricated by coating a glass-slide with Primer G and adding a thin-layer of MY-132A of around 1 mm thickness. After reapplication of Primer G the pillar-structure of MY-133-V2000 was added by injection molding.

For the measurements, optical fibers were placed at the two ends of the central, straight part of the pillar-structure like it is shown in Figure 7 a). Alignment of the fibers at the front- and end-cleavage was achieved with two piezo-stages. The spectral response was obtained by connecting a halogen-lamp and measuring transmission with the spectrometer QE65000 from Ocean Optics.

The pillar-structure exhibits the typical appearance of a waveguide with light only visible at the front- and end-facet due to scattering. The intensity of theses two spots especially at the right (output) facet suggests a lot of insertion losses, which is owed to the difference in size and shape. Fibers and pillar have the same height, but the pillar has more than four times their width. So especially coupling from the pillar to the output fiber a lot of intensity is lost.

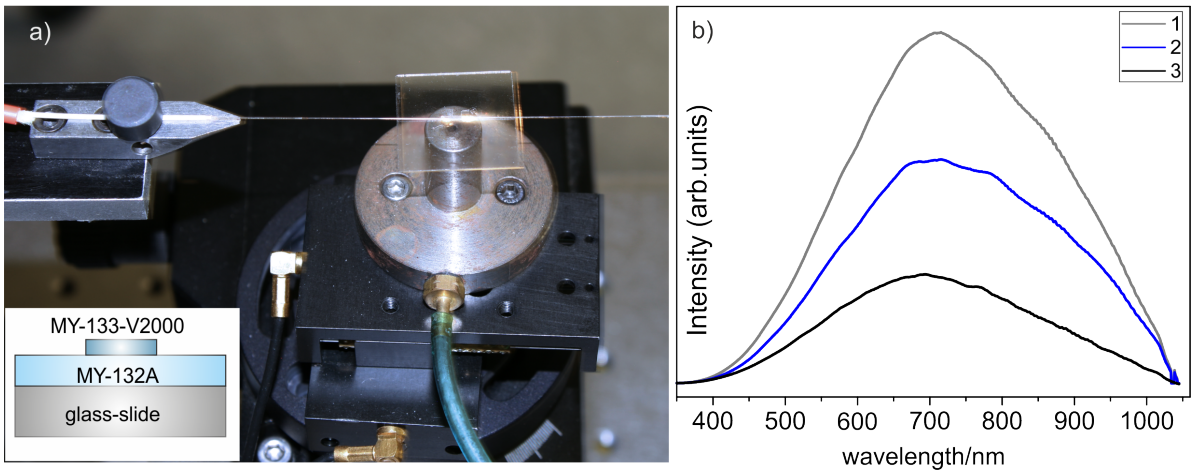

Figure 7. a) Photograph of the setup showing the input and output fiber optics with the pillar-structure (the inset contains a scheme of the composition) in the middle and the light source turned on. b) Transmission measurement of the setup in a) for the three cases: Fibers in constant distance and 1. waveguide with air-cladding, 2: waveguide with water-cladding, 3: no waveguide in between.

Transmission was measured with air and distilled water as upper cladding of the model WG and in the case of its removal from between the fiber optics. The RI of air is 1 and the RI of distilled water is about 1.33 in the visible. As the latter is matching the RI of the waveguide material MY-133-V200 (n = 1.333), confinement inside the structure should be high for the air-cladding. Hence, one expects the intensity reaching the second fiber to be highest for the waveguide with air as upper cladding in between and to drop subsequently in the case of water covering the pillar structure and removal of the waveguide. In the case of the water cladding, the transmitted intensity depends on the degree of confinement. The results are plotted in Figure 7 b).

As expected, for the waveguide with air cladding, the intensity reaching the output fiber was the highest. Removing the waveguide, the intensity dropped drastically. To realize the water cladding, which is more similar to the real case, a droplet of distilled water was placed on top of the pillar structure without touching the fiber optics. Intensity dropped to a level just around the middle of that in the two other cases, which means some degree of leakage, but still a reasonable amount of signal reaching the output.

Of course the dimensions of this experiment are not comparable with the real application and the results are therefore no quantitative measures. Still, confinement has been demonstrated with a RI-matching model, and the MY-132A proved suitable as support-material.

4. Conclusions

The requirements for the implementation of mono-layers of vascular ECs as living WGs have been investigated and solutions for the main problems, i. e. materials and coupling,

have been developed. The issue of the low refractive index of vascular ECs has been tackled by the investigation of novel materials with even lower RI. Micro-structuring using soft-lithography as well as first confinement tests have shown positive results. To make efficient coupling to LWGs possible, a tapered waveguide performing the necessary mode-conversion has been designed. Combining a micro-fluidic part made of the new material and the optics designed for coupling such that the vascular ECs form a mono-layer connecting the optic input and output, a cell-based lab-on-chip with cells in the dual role of transducer and reporter has been designed. Future research will concentrate on the fabrication and bringing into service of the lab-on-chip.

Acknowledgements

This research was carried out as part of the LiPhos project, which is partly funded by the European Commission (Contract No. 317916). I would like to thank Sandra de Pedro Jordan, Jordi Vila Planas and Alfredo Abelardo Gonzáles Fernández for their advise, Dr. Andreu LLobera Adán for his help and many fruitful discussions and especially Dr. Xavier Muñoz Berbel for the supervision and excellent guidance during this work.

References

[1] Nichols M, Townsend N, Luengo-Fernandez R, Leal J, Gray A, Scarborough P, Rayner M 2012 *European Cardiovascular Disease Statistics* (Brussels: European Heart Network, European Society of Cardiology, Sophia Antipolis) ISBN 9782953789812 URL http://www.ehnheart.org/cvd-statistics/cvd-statistics-2012.html

[2] Razzouk L, Fusaro M and Esquitin R 2012 *Current cardiology reviews* **8** 109–15 ISSN 1875-6557

[3] Van Holten T C, Waanders L F, De Groot P G, Vissers J, Hoefer I E, Pasterkamp G, Prins M W J and Roest M 2013 *PloS one* **8** e62080 ISSN 19326203

[4] Wang J, Wu C, Hu N, Zhou J, Du L and Wang P 2012 *Biosensors* **2** 127–170 ISSN 2079-6374

[5] Young E W K and Simmons C a 2010 *Lab on a chip* **10** 143–60 ISSN 1473-0197

[6] Larrivée B and Karsan A 2005 *Methods in molecular biology (Clifton, N.J.)* **290** 315–29 ISSN 1064-3745 URL http://www.ncbi.nlm.nih.gov/pubmed/15361671

[7] Okamoto K 2006 *Fundamentals of optical waveguides* 2nd ed (Elsevier) ISBN 0-12-525096-7

[8] Yashunsky V, Marciano T, Lirtsman V, Golosovsky M, Davidov D and Aroeti B 2012 *PloS one* **7** e48454 ISSN 1932-6203

[9] 2013 My polymers ltd. URL http://www.mypolymers.com/products